Biological Trace Element Research (2019) 187:392–402
https://doi.org/10.1007/s12011-018-1392-0

Green Engineered Biomolecule-Capped Silver Nanoparticles Fabricated from *Cichorium intybus* Extract: In Vitro Assessment on Apoptosis Properties Toward Human Breast Cancer (MCF-7) Cells

Sorayya Behboodi[1] · Fahimeh Baghbani-Arani[2] · Sahar Abdalan[2] · Seyed Ataollah Sadat Shandiz[3]

Received: 20 March 2018 / Accepted: 18 May 2018 / Published online: 28 May 2018

Abstract
The current experiment reveals the anticancer properties of silver nanoparticles (AgNPs) synthesized using aqueous leaf extract of *Cichorium intybus,* a significant medicinal plant. The characteristics of AgNPs were continuously studied by powder X-ray diffraction (XRD), Fourier-transform infrared spectroscopy (FTIR), zeta potential, transmission electron microscopy (TEM), scanning electron microscopy (SEM), and energy-dispersive spectroscopy (EDS) analysis. Current microscopic results show that produced AgNPs were spherical in shape with an average size of 17.17 nm. A strong peak between 2 and 4 keV showed the greatest ratio of the elemental silver signals, due to surface plasmon resonance (SPR). The AgNPs, fabricated by green method, had a negative zeta potential of − 9.76 mV, which indicates that the synthesized AgNPs is dispersed in the medium with high stability. The in vitro cytotoxicity effect of AgNPs showed promising anticancer activity against human breast cancer MCF-7 cells. Annexin V-FITC/propidium iodide assay, Hoechst 33258 staining, and upregulation of caspase 3 activity revealed significant apoptosis activities of AgNPs against MCF-7 cells. Moreover, the flow cytometric analyses of cell cycle distribution of MCF7 cells showed that AgNPs treatment has enhanced the sub-G1 peaks, which is an indicator of apoptosis pathway. Overall results in our study suggested that AgNPs fabricated by a biogreen approach could be useful in cancer therapy.

Keywords Apoptosis · *Cichorium intybus* · Green synthesis · AgNPs · MCF-7

Introduction

The fabrication and characterization of nanoparticles, particularly from metals such as platinum, silver, gold, and palladium, have gained wide interest due to their significant application in bioengineering, nanotechnology, medicine, electronics, optoelectronics, and making advancement in various fields [1–3]. Among the noble metallic nanoparticles, silver nanoparticles (AgNPs) have received a wide interest due to their chemical and physical properties [4]. Numerous chemical and physical techniques have also been used for the preparation of silver nanoparticles; nevertheless, these strategies are expensive and possibly pollute the environment due to usage of harsh reagents [5]. Therefore, it is desirable to improve simple and eco-friendly synthesis strategies for fabrication of greener metal nanoparticles with high purity. Biological synthesis of nanoparticles is eco-friendly and environmentally benign method for fabrication of nanoparticles. In this regard, there are number of different plants that have been successfully used for fabrication of AgNPs, including *Azadirachta indica* [6, 7], *Tephrosia purpurea* [8], *Glycyrrhiza glabra* [9], *Gongronema latifolium* [10], and *Diospyros paniculata* [11]. On the basis of different reports on green synthesis, we introduced a swift route of phytosynthesis of silver nanoparticles using the leaf extract of *Cichorium intybus.* The genus *Cichorium* belongs to family Asteraceae, and it is found abundantly in tropical Asia, North Africa, and Europe [12]. *C. intybus* plant extract as a traditional medicine is employed for different purposes including liver rejuvenation, skin aliment treatment [13], wound healing [14], antimicrobial [15], and antimalarial activities [16].

✉ Seyed Ataollah Sadat Shandiz
Ata.sadatshandiz@iauctb.ac.ir

[1] Department of Biology, Tehran Shargh, Payam Noor University, Tehran, Iran

[2] Department of Genetics and Biotechnology, School of Biological Science, Varamin-Pishva Branch, Islamic Azad University, Varamin, Iran

[3] Department of Biology, Central Tehran Branch, Islamic Azad University, Tehran, Iran

According to previous phytochemical studies, several compounds exist in *C. intybus* plant extract which includes a large number of phenolic acids, triterpenoids, sterols, and hydroxycinnamic acid derivatives [17–19], which might be introduced to bioreduction of silver ions to fabricate AgNPs.

The aim of the current study was to green synthesize a stable AgNPs by using *C. intybus* extract. The fabricated AgNPs were characterized using different spectroscopic and microscopic techniques such as EDS, XRD, SEM, TEM, zeta potential, and FTIR analysis. The final goal of this study was to investigate the mechanism of green-assisted synthesis of AgNPs-induced apoptosis in human breast MCF-7 cancer cells.

Material and Methods

Preparation of Extract and Green Synthesis of AgNPs

The collected fresh leaves of *C. intybus* were washed thoroughly and air-dried in the shade at room temperature and made into fine powder using a mixer. About 20 g of dried healthy leaf powder was extracted by boiling in 200 ml of double distillated water for 1 h and separated by Whatman No. 1 filter paper (Whatman plc, Maidstone, Kent, UK) and used for further characterization study. To synthesize AgNPs, 4 ml of the filtrate extract was treated with 100 ml of 0.01 mM of silver nitrate ($AgNO_3$) solution with continuous stirring at room temperature for 1 h. After completion of the reaction, the reaction mixture was transferred into 50 ml falcon tube and centrifuged (ROTANTA 460 centrifuges, Sigma-Aldrich) at 17,004×*g* for 30 min followed by three times washing with sterile distilled water.

Characterization of Fabricated AgNPs

The visual observations of AgNPs using *C. intybus* extract were performed to monitor the conversion of Ag ion into Ag nanoparticles. The produced AgNPs size and morphology were identified under field transmission scanning electron microscope (SEM) and transmission electron microscopy (TEM) images were recorded by Carl Zeiss Meditec AG, Jena, Germany. An energy-dispersive spectroscopy (EDS) analysis was examined to confirm the chemical composition of fabricated AgNPs. The crystallographic nature of the prepared AgNPs was evaluated using X-ray diffractometer instrument (PANalytical X'PertPro MPD, PANalytical, Almelo, The Netherlands) in the range of 2θ from 10 to 100 °C, Cu Kα radiation at 40 kV and 30 mA. FTIR spectroscopy measurements were performed to analyze the absorption of possible organic compounds on the fabricated AgNPs surface. The FTIR spectra of AgNPs were recorded in the range of 4000 and 400 cm^{-1} in KBr pellets using FTIR spectrophotometer (Perkin Elmer RX1, Spectrum Two Germany). Thereafter, measurement of zeta potential of produced nanoparticles was performed by Malvern Zetasizer (Malvern instrument Ltd., Worcestershire, UK).

Cell Culture Conditions and Cell Viability Determination

The human breast cancer (MCF-7) cells were obtained from the National Cell Bank of Iran (NCBI)-Pasteur Institute of Iran. For culture maintenance, the cells were cultured on standard Dulbecco's modified Eagle's medium (DMEM) with 10% fetal bovine serum (FBS), 100 μg/ml streptomycin, and 100 units/ml penicillin solution at 37 °C in the presence of 5% humidified CO_2 in air. MCF-7 cell viability examination was measured by performing MTT [3-[4,5-dimethylthiazol-2-yl]-2,5-diphenyltetrazolium bromide] colorimetric assay. Approximately, 1×10^4 cells were plated in each well of a 96-well plate and cultured for 24 h. Thereafter, the MCF-7 cells were exposed to series of 3.90–1000 μg/ml concentrations of AgNPs at 37 °C in the presence of 5% humidified CO_2 for 24 h. The untreated cancer cells were assayed as control. After completion of incubation time, the untreated and AgNPs-treated cells were incubated by 100 μl MTT solution (0.5 mg/ml) at the same condition for 4 h. In each well, 100 μl of dimethyl sulfoxide (DMSO) was added to dissolve the formazan crystal formed in the reaction. The optical density (OD) of purple blue formazan dye was determined at 570 nm in an ELISA plate reader (UV-1601, Shimadzu, Kyoto, Japan). The ratios of OD value of treated AgNPs samples to the untreated samples were used to calculate the percentage of cell viability.

Caspase 3 Activity Assay

The activity of caspase 3 was evaluated using test kit following the manufacturer's protocol (Apo*Target*™ Caspase assay, Invitrogen Corp, Camarillo, CA, USA). In brief, the MCF-7 cells were seeded in 6-well plate and treated with AgNPs. At the end of 24 h incubation, the cells were incubated on caspase 3 assay reagents and incubated for 2 h in dark room. Finally, the absorbance was measured at 400 or 405 nm using a microplate autoreader (Bio-Tek Instruments, Inc., Vinooski, VT, USA). The caspase 3 activity of treated cells was calculated by comparing these data with the level of the untreated cell groups.

Hoechst Staining

MCF-7 cells (4×10^5cells per well) were grown in 6-well tissue culture plate and were allowed to stand and by incubated at 37 °C for 24 h. Cells were treated by AgNPs and were further incubated at 37 °C for 24 h. After that, cells

were stained with Hoechst 33258 dye (5 μg/ml), and incubated in the dark. Live and apoptotic cells were distinguished under fluorescent microscope (Nikon TI 2000, Nikon, Okinawa, Japan).

Annexin V-FITC/Propidium Iodide Staining

Analyses of apoptotic and necrotic cells were performed by annexin V-FITC/PI staining as described previously [20]. Briefly, the cells were treated with produced AgNPs and centrifuged, stained with annexin V-FITC and PI staining kit, and evaluated by flow cytometry (Cyflow, UK). Flow cytometry analysis of annexin V-FITC/propidium iodide apoptosis assay was determined to quantify necrotic, early apoptotic, late apoptotic, and viable cells.

Cell Cycle Analysis

Cell cycle distribution was determined by the assessment of DNA contents based on fluorescence intensity. Briefly, MCF-7 (1×10^6 cell/ml) cells were seeded onto 6-well plate and were allowed to attach overnight. Following incubation, the cells were treated at respective IC_{50} dose of AgNPs for 24 h. Then, the cells were pelleted, washed with PBS, and fixed in cold 70% ethanol for 30 min at 4 °C. The fixed cells were centrifuged at 2000 rpm and resuspended in PBS containing RNase (100 μg/ml), followed by staining with propidium iodide for at least 1 h in the dark to stain DNA. Finally, the DNA content was measured by flow cytometry (Cyflow, UK).

Statistical Analysis

All data were analyzed using one way analysis of variance (ANOVA) with the post hoc test employing SPSS 10.0. Statistical significance was determined when P value was less than 0.05.

Result and Discussion

Characterization of Silver Nanoparticles

The current research focused on fabrication of green engineered biomolecule-loaded AgNPs and to determine their anticancer properties against breast cancer cell line. Recently, many reports have highlighted that the green synthesized metal nanoparticles fabricated from plant extracts have a promising cytotoxicity effect against tumor cells due to the presence of secondary metabolites of plants for stability of nanoparticles [21–23]. There are limited investigations on the production of nanoparticles with the aid of *Cichorium* species and this is the first work to report the apoptotic activity of AgNPs synthesized using *Cichorium intybus* leaf extract against breast cancer MCF-7 cell line. Gallucci et al. fabricated silver nanoparticles of 19 to 64 nm size using leaf extract of Belgian endive, a variety of *Cichorium intybus* L. and indicated their antibacterial activities [24]. In our study, the apoptotic properties of AgNPs derived from extract were investigated using the reaction containing AgNPs in the presence of *C. intybus* extract as the stabilizing and reducing agent. The visual observation was monitored by $AgNO_3$/extract solution for 24 h. The change in reaction solution into reddish brown solution from colorless $AgNO_3$ solution at the end of 24 h indicates the reduction of Ag^+ into AgNPs (Fig. 1). FTIR measurements of fabricated AgNPs and extract were performed to ascertain the possible functional groups of the extract responsible for the stabilizing and fabrication process of *C. intybus*-mediated AgNPs. FTIR bands for *Cichorium intybus* extract were obtained at 3414.03, 2933.04, 1612.78, 1420.11, 1267.04, 1122.68, 1053.73, and 604.30 cm^{-1} (Fig. 2). Through FTIR spectrum of AgNPs, the broad band at 3413.05 cm^{-1} suggests the presence of O–H alcohol functional group. Peak at 2922.98 cm^{-1} corresponds to aliphatic C–H group, while peaks at 1619.08 cm^{-1} and 1384.60 cm^{-1} are assigned to C=C and C–H bend alkane groups, respectively. Peak at 1114.28 cm^{-1} associated with C–O–C stretch ethers, while 874.47 cm^{-1} represents N–H functional groups. Functional groups such as terpenoids and phenols are responsible for bioreduction and fabrication of capping layers on the synthesized AgNPs. Previous published reports also observed similar peaks of silver nanoparticles's FTIR spectrum [25, 26]. To obtain information regarding the size and morphology of the AgNPs, it was characterized by FESEM images. It is obvious from Fig. 3 that the distribution pattern of synthesized Ag nanoparticles was predominantly spherical-shaped particles. From the transmission electron microscope (TEM) images in Fig. 4, the *Cichorium intybus*-mediated AgNPs were homogeneous and spherical in shape with an average diameter ranging from 5 to 30 nm. The size of the histogram in Fig. 4d shows that most of the AgNPs have an average size of 17.17 nm. Data obtained from EDX analysis confirmed the presence of silver elemental signals in the produced AgNPs (Fig. 5). A strong peak between 2 and 4 keV showed the greatest ratio of the elemental silver signals, due to surface plasmon resonance (SPR) [21]. The other weak signals such as carbon and oxygen in the EDS profile confirmed the presence of organic moieties in plant extract, which are adsorbed on the surface of the fabricated AgNPs.

To validate the green synthesis of *Cichorium intybus* silver nanoparticles and further analyze the crystalline nature of AgNPs, XRD was performed by investigating their intensities of various diffracted beams and calculating the angles. Regarding the crystallographic structure of the AgNPs

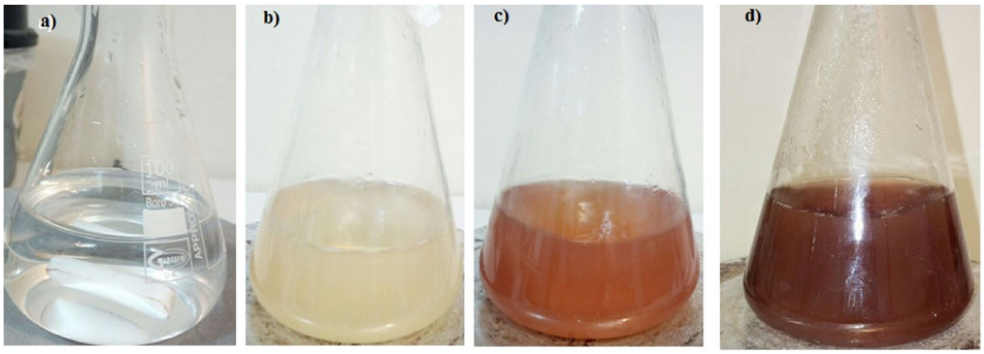

Fig. 1 *Cichorium intybus*-mediated green synthesis indicating color changes after adding the plant extract. A total of 0.01 Mm of silver nitrate solution before adding the *Cichorium intybus* extract (**a**), and after treatment with *Cichorium intybus* extract during 2 h (**b**), 12 h (**c**), and 24 h (**d**)

synthesized by *Cichorium intybus* extract, four intense XRD peaks were indicated, corresponding to the (111), (200), (220), and (311) crystallographic planes of face-centered cubic (fcc) structure at 2θ angles of 38.6, 44.4, 64.6, and 77.1, respectively (Fig. 6). Zeta potential measurement was used to calculate the net charge of resultant AgNPs. The AgNPs, fabricated by green method, had a negative zeta potential of − 9.76 mV (Fig. 7), which indicates that the synthesized AgNPs are dispersed in the medium with high stability.

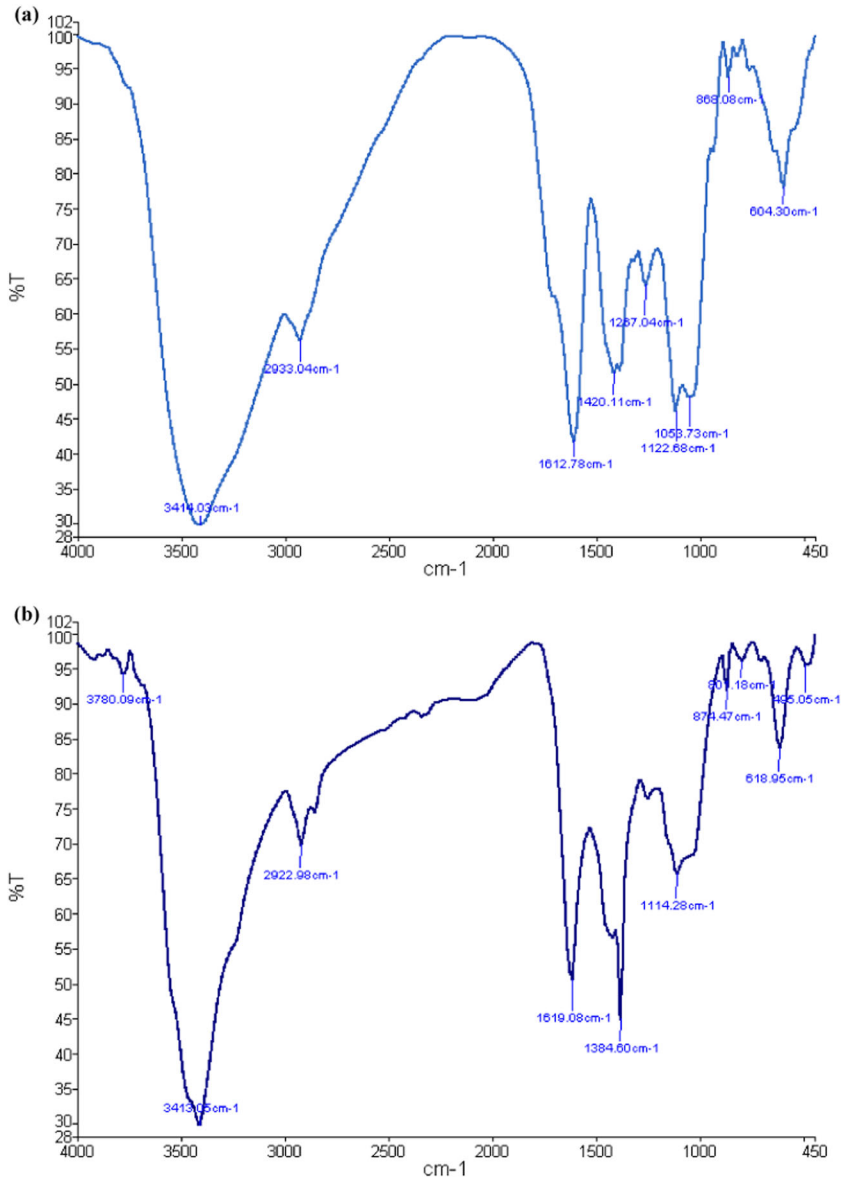

Fig. 2 FTIR spectra of **a** *C. intybus* extract and **b** green synthesized *C. intybus*-AgNPs

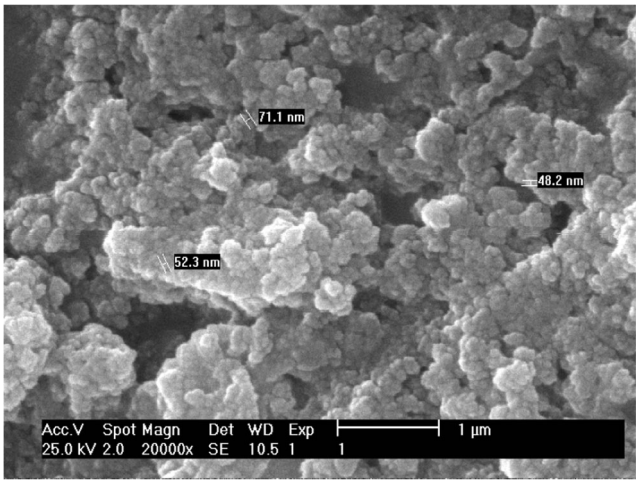

Fig. 3 FESEM image of AgNPs synthesized using *C. intybus* extract

In Vitro Cytotoxicity of AgNPs

Treatment of MCF-7 cells at different concentrations of AgNPs 3.90, 7.81, 15.62, 31.25, 62.5, 125, 250, 500, and 1000 µg/ml was measured by the cytotoxicity MTT assay within 24 h. According to the data in Fig. 8, it can be indicated that the cell line cytotoxicity has dose-dependent manner. After increasing the concentration of AgNPs, the cell viability was decreased. The produced AgNPs at 1000 µg/ml concentration exhibited 85% inhibition of MCF-7 cell proliferation, which was significantly different with the untreated cells as control group ($P < 0.001$). However, the lowest suppressions in cell growth at 3.90, 7.81, 15.62, 31.25, and 62.5 µg/ml concentrations indicated no significant differences in comparison with the control group ($P > 0.05$). In addition, half maximal growth inhibitory concentration

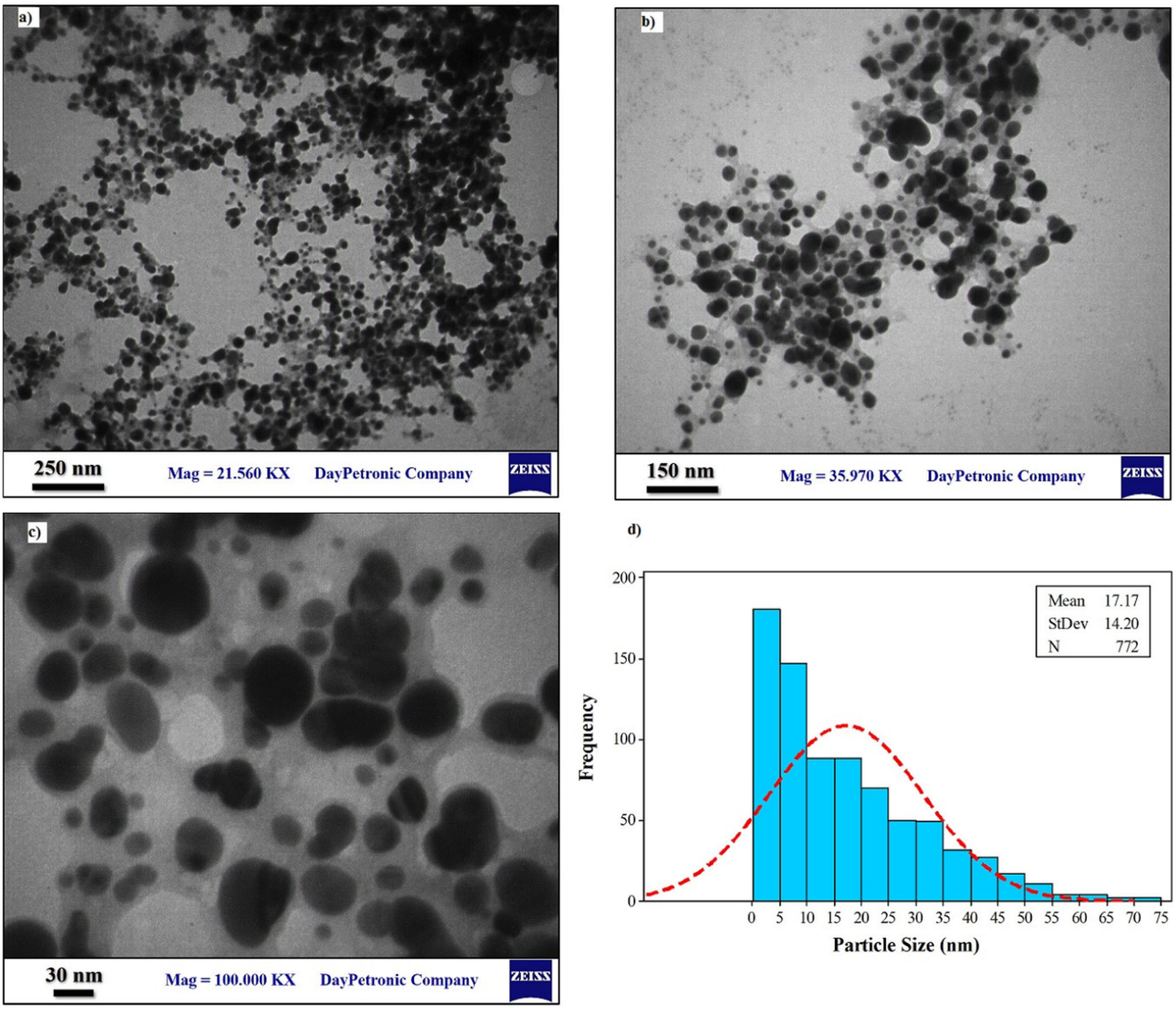

Fig. 4 TEM images of AgNP-*C. intybus* in different magnifications (**a**–**c**), and histogram of particles size (**d**)

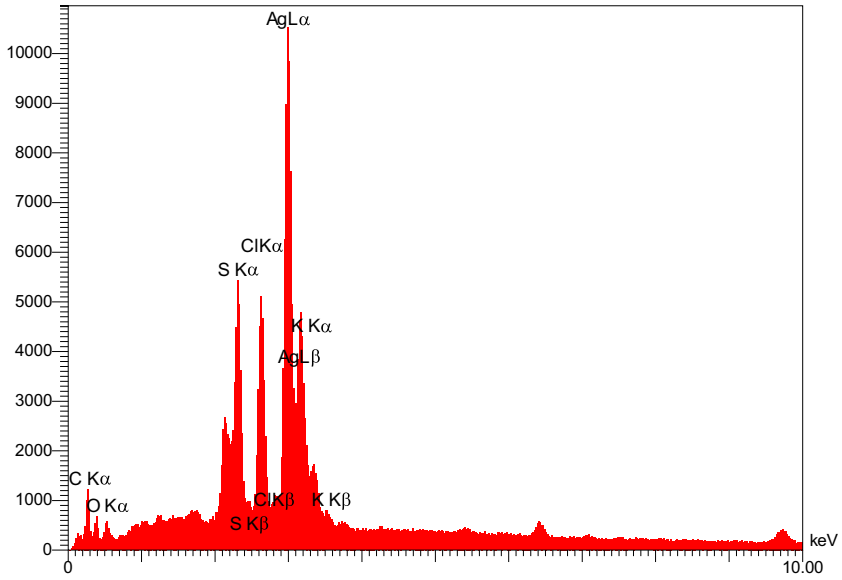

Fig. 5 EDX spectrum of the green synthesized AgNPs. A strong peak at ~ 3 keV indicates the greatest ratio of the elemental Ag signals

(IC_{50}) value measured for MCF-7 cells was 507.58 μg/ml for AgNPs after 24 h. Different factors such as shape, size, composition, surface hydrophobicity, and surface charge of nanoparticles are respectively important aspects that affect the cytotoxicity of nanoparticles [27]. A significant number of investigated in vitro studies have detected the cytotoxicity of silver nanoparticles on different cancer cell lines. Abd Kelkawi et al. indicated the dose- and cell line-dependent cytotoxicity effect of AgNPs using *Mentha pulegium* extract on HeLa and MCF-7 cancer cell lines. More than 58 and 47% mortalities were observed after 48 h exposure of MCF-7 and HeLa cells, respectively, to 100 μg/ml AgNPs [28]. Potential anticancer properties of AgNPs from *Chaenomeles sinensis* extracts were reported against MCF-7 cells [29]. Ag^+ ions released from AgNPs could contribute to cell cytotoxicity via different damaging mechanisms such as decrease cell membrane integrity and enhanced permeability, and they can increase in cell apoptosis induced by the DNA damaging. Also, silver ions bind to thiol groups in proteins, resulting in protein deactivation. Moreover, recent reports suggest that green synthesized silver nanoparticles can trigger cell growth by the generation of reactive oxygen species (ROS) [30, 31]. Abundance of ROS can affect the different processes in cells such as alteration in gene expression, DNA

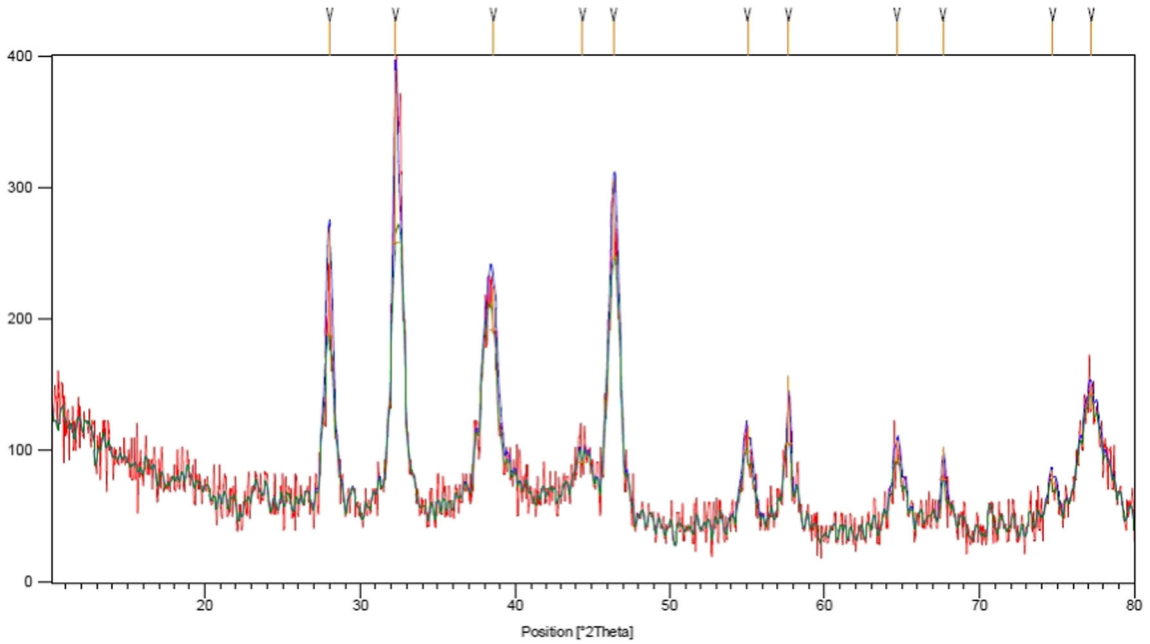

Fig. 6 XRD pattern of AgNPs synthesized using *C. intybus* extract

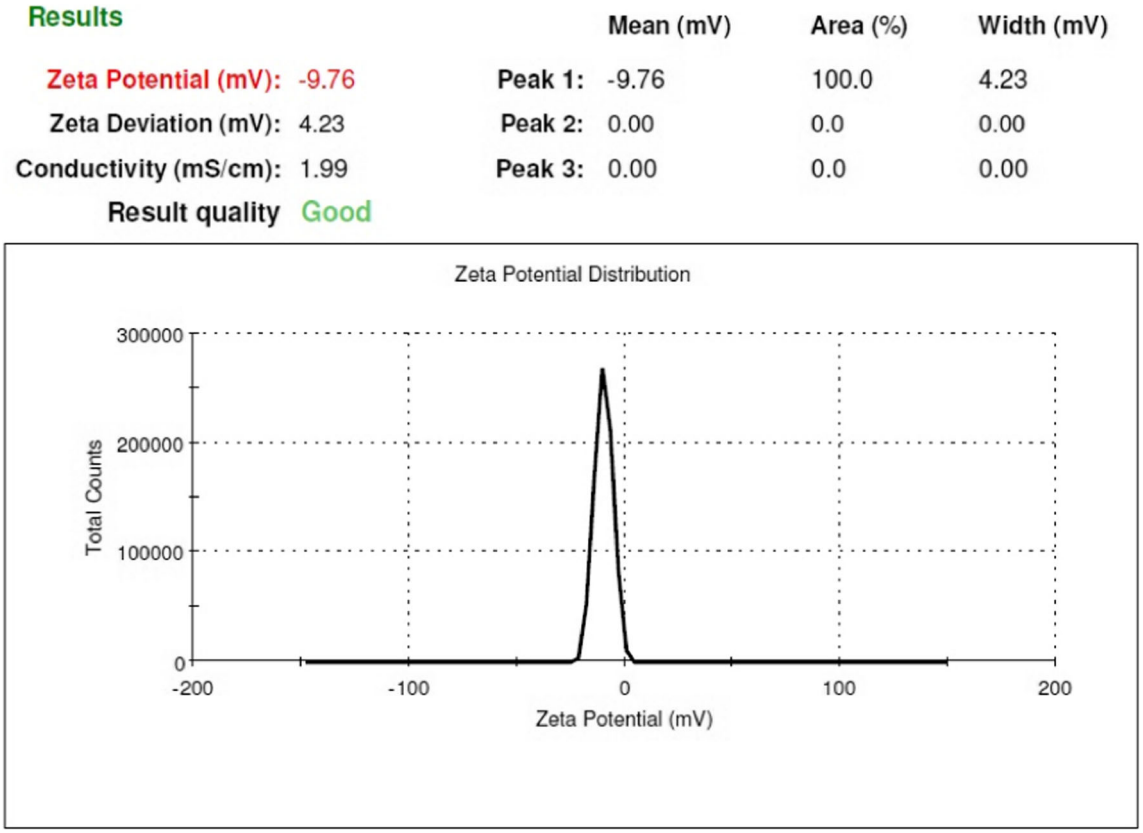

Fig. 7 Zeta potential of synthesized AgNPs fabricated using aqueous leaf extract of *Cichorium intybus*

damage, activation of transcription factors, and promotion of apoptosis signal transduction pathway [32]. Aceituno et al. and his team showed that the silver nanoparticles from *Dendropanax morbifera* Léveille leaves reduced cell proliferation and enhanced ROS production in A549 and HepG2 cancer cell lines. They reported that ROS generation induced by green synthesized silver nanoparticles might be related to modification of the p38 MAPK pathway. They also reported that the silver nanoparticles enhanced the *Bax*, and decreased *Bcl-2* gene expressions and increased the percentage of apoptotic A549 cells [33].

Determination of Apoptotic Effects in MCF-7 Cells

Currently, the functions of most anticancer therapeutic agents were to kill the cancer cells by activation of apoptosis

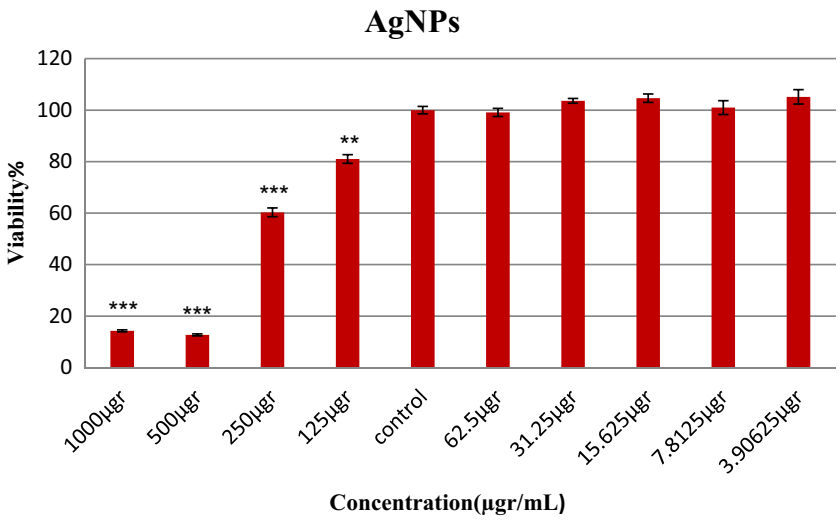

Fig. 8 Viability percentage of the breast cancer MCF-7 cells after incubation for 24 h with various concentrations of the AgNPs

[34]. Apoptotic pathway is basically regarded as a programmed cell death, which includes several changes in morphology of the cells, including activation of caspases, chromatin condensation, DNA, and nuclear fragmentation [35, 37]. In order to explore the effect of AgNPs on cell death in MCF-7 cells, we determined cell nuclear morphology with Hoechst staining after 24 h treatment. As shown in Fig. 9, AgNPs-treated MCF-7 cells show an increase in the apoptotic features like apoptotic bodies and nuclear condensation, while a few apoptotic characteristics were observed in the untreated cells (control group). Recently, many investigations suggest that silver nanoparticles can initiate apoptosis pathway via apoptotic body, chromatin condensation, and formation of DNA fragmentation in different cancer cell lines including Ehrlich's ascites carcinoma (EAC) cells [36, 38], A549 lung cancer cell line [39], breast cancer MCF7, and MDA-MB-231 cell lines [40].

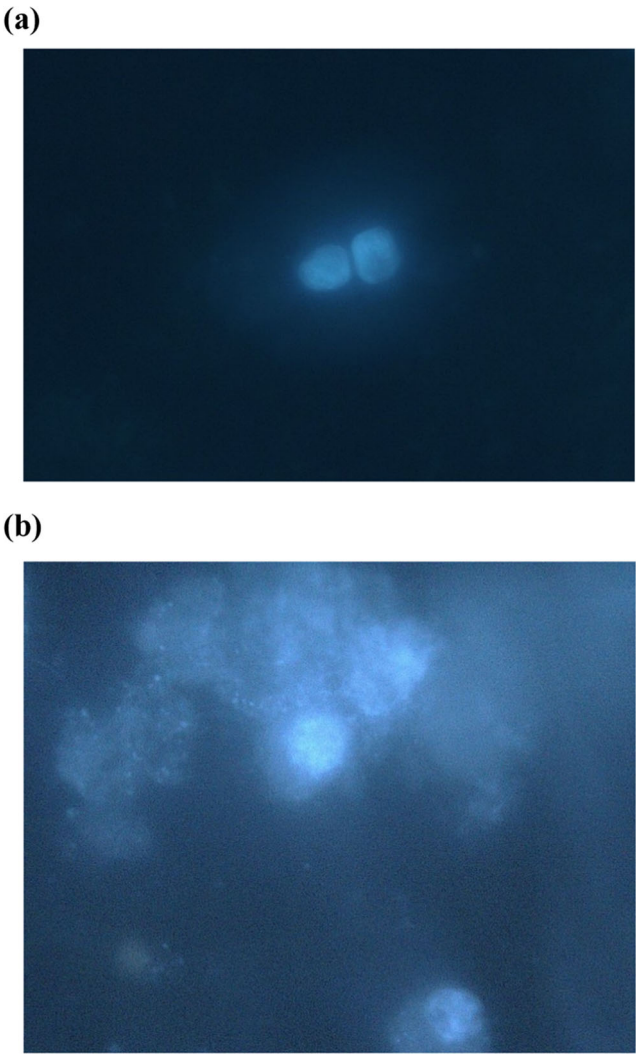

Fig. 9 Photographic record of Hoechst-stained apoptotic cells after AgNPs treatment of MCF-7 cells. Here, **a** untreated MCF-7 cells and **b** MCF-7 cells treated with AgNPs (507.58 μg/ml)

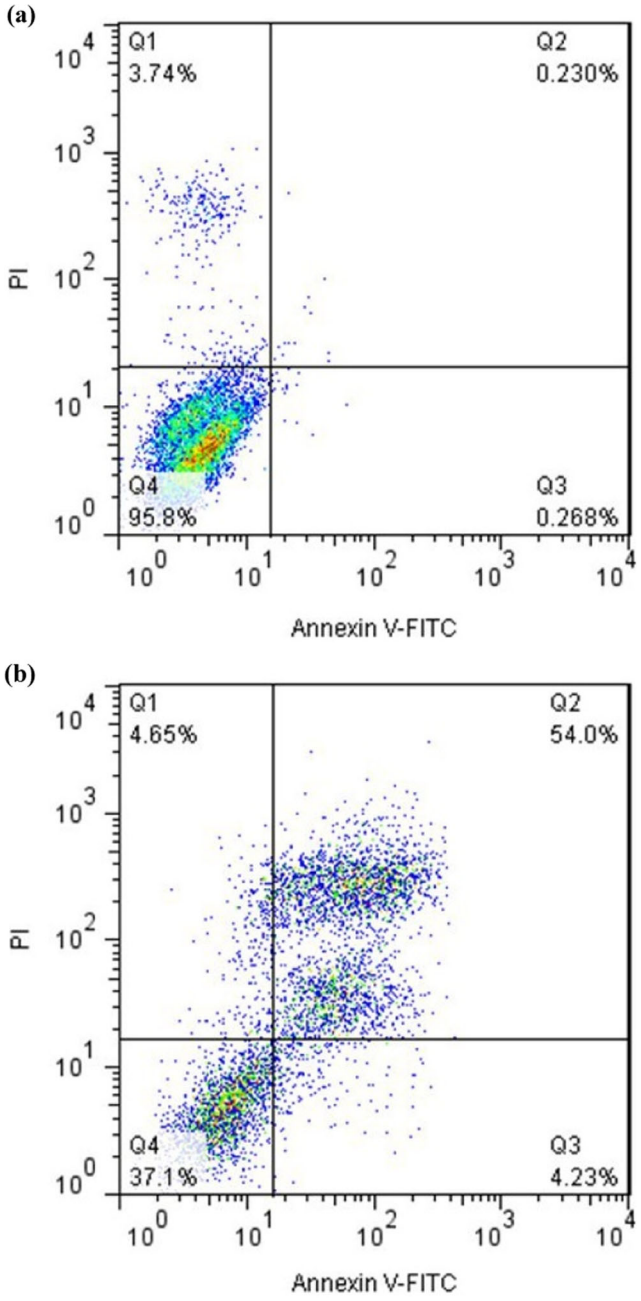

Fig. 10 Flow cytometric analysis by annexin V-FITC/PI staining. **a** Untreated MCF-7 cells. **b** AgNPs-treated cells. MCF-7 cells with annexin V-FITC−/PI− (lower left quadrant), considered as viable cells. Cells with annexin V-FITC−/PI+ (upper left quadrant) was indicated as necrotic cells. The lower right quadrant (annexin V-FITC+/PI−) was labeled as early apoptotic cells, and the upper right quadrant (annexin V-FITC+/PI+) was represented late apoptotic MCF-7 cells

In comparison to apoptosis, necrosis, a pathological cell death, is characterized by nuclear dissolution, inflammatory, cell swelling and scarring [41, 42]. Triggering cell death aid by apoptosis pathway plays a crucial role in cancer therapy approaches [43]. In this study, the percentage of apoptotic and necrotic cells due to AgNPs treatment was evaluated by an annexin V-FITC/propidium iodide apoptosis assay. As

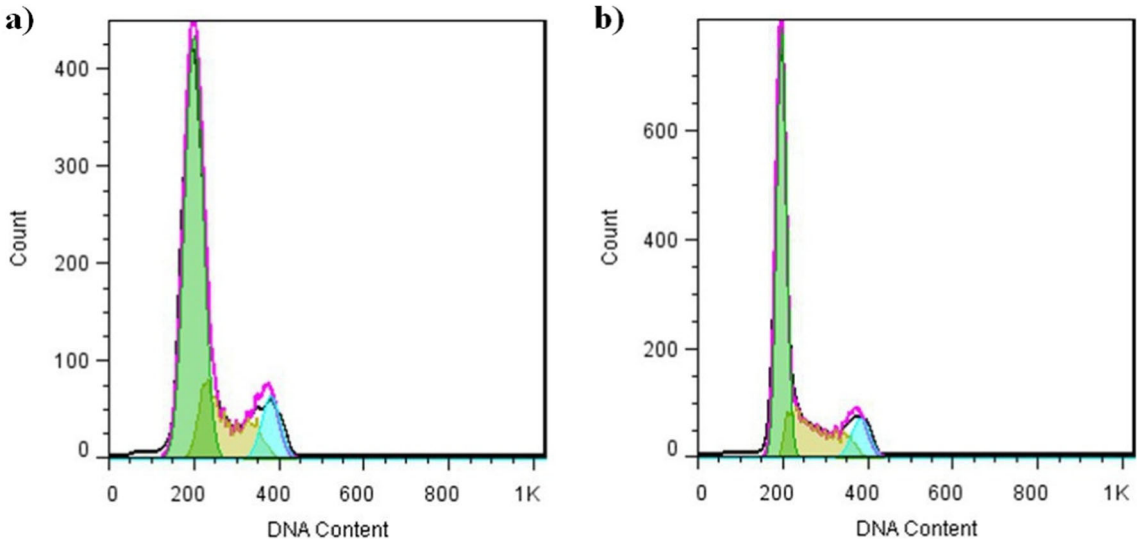

Fig. 11 The flow cytometric analyses of cell cycle distribution in MCF-7 cells **a** without treatment (control) and **b** after treating with AgNPs for 24 h

depicted in Fig. 10, the upper left quadrant (Q1) and lower left quadrant (Q4) depict the percentage of necrotic and viable cells, respectively. Nevertheless, the Q2 (upper right quadrant) and Q3 (lower right quadrant) represent the percentage of early and late apoptotic cells, respectively.

After 24 h exposure to AgNPs, flow cytometry analysis of annexin/PI staining in untreated and treated MCF-7 cells is shown in Fig. 10. MCF-7 cells treated with AgNPs had 4.23% early stage apoptosis and 54% late stage apoptosis, compared to untreated ones in MCF-7 cell line. In our previous study, we indicated the AgNPs produced using *Artemisia tournefortiana* Rchb cytotoxicity against human colon cancer HT29 cells. Approximately, 11 and 9% enhancement was shown in early and late apoptosis in the cancer cells [20]. However, in our work, MCF-7 cells exposed to AgNPs had 4.23 and 54 % in early and late stage of apoptosis, respectively. In accordance with the annexin V/PI assay result, cell death including apoptosis, not necrosis, was the main route in AgNPs-activated cytotoxicity. To extend our studies about apoptotic effects of AgNPs, the flow cytometric analyses of cell cycle data in cancer cells exposed to AgNPs were investigated. As shown in Fig. 11a, untreated cells revealed healthy growing cells, while AgNPs-treated cells indicated an enhancement in the cell population at sub-G1 phase which led to triggering of apoptosis pathway in cells.

We further expanded the apoptotic activity of our nanoparticles by determining a mechanism involving the apoptotic pathway in AgNPs-induced caspase 3 response in MCF-7 cells. Caspases are aspartate-specific cysteine protease enzymes that have significant role in regulation of apoptosis pathway. It was confirmed that caspase 3 proteins have a significant role in nuclear morphological and biochemical changes in apoptotic cells [44, 45]. Figure 12 shows the increase in the levels of caspase 3, a pro-apoptotic marker, the activity of

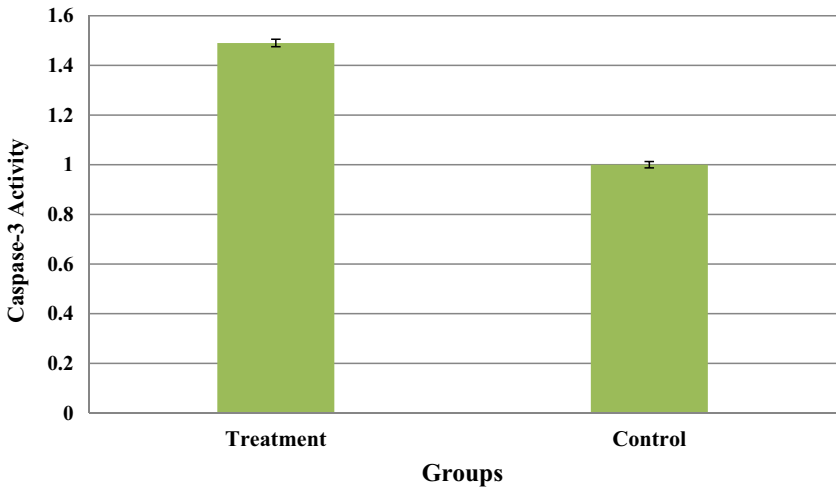

Fig. 12 The activity of caspase 3 was enhanced after AgNPs-exposed MCF-7 cells, which indicates that apoptosis pathway

nanoparticle-exposed cancerous cells, showed that AgNPs execute cell death by triggering apoptosis cascade. Baharara et al. [46] reported the apoptotic potential of silver nanoparticles fabricated with *Zataria multiflora* leaf extract in HeLa cells. They showed an enhanced level of caspase 3/9 activation in the cancerous cells.

Conclusions

This work proposed the simple cost-effective and eco-friendly green synthesis of AgNPs using the aqueous extract of *C. intybus*. As observed from TEM micrograph, spherical-shaped AgNPs have an average size of 17.17 nm. The produced AgNPs showed promising in vitro cytotoxic activity against human breast cancer MCF-7 cells. Enhancement in caspase 3 activity, cell cycle arrest in subG1 phase, and increase in the nuclear fragmentation features in AgNPs-exposed MCF-7 cells suggest the possible impact of AgNPs in inducing apoptosis pathway. In conclusion, the produced AgNPs triggered potent anticancer activity toward MCF-7 cancer cells, suggesting their significance for different pharmaceutical and biomedical applications.

Compliance with Ethical Standards

Conflict of Interest The authors declare that they have no conflicts of interest.

References

1. Murugan K, Benelli G, Ayyappan S, Dinesh D, Panneerselvam C, Nicoletti M, Hwang JS, Kumar PM, Subramaniam J, Suresh U (2015) Toxicity of seaweed-synthesized silver nanoparticles against the filariasis vector *Culex quinquefasciatus* and its impact on predation efficiency of the cyclopoid crustacean *Mesocyclops longisetus*. Parasitol Res 114:2243–2253
2. Parameshwaran R, Kalaiselvamb S, Jayavel R (2013) Green synthesis of silver nanoparticles using *Beta vulgaris*: role of process conditions on size distribution and surface structure. Mater Chem Phys 140:135–147
3. Aarthi C, Govindarajan M, Rajaraman P, Alharbi NS, Kadaikunnan S, Khaled JM, Mothana RA, Siddiqui NA, Benelli G (2017) Eco-friendly and cost-effective Ag nanocrystals fabricated using the leaf extract of *Habenaria plantaginea*: toxicity on six mosquito vectors and four non-target species. Environ Sci Pollut Res 25:10317–10327. https://doi.org/10.1007/s11356-017-9203-2
4. Kim JS, Kuk E, Yu KN, Kim JH, Park SJ, Lee HJ, Kim SH, Park YK, Park YH, Hwang CY, Kim YK, Lee YS, Jeong DH, Cho MH (2007) Antimicrobial effects of silver nanoparticles. Nanomed Nanotechnol Biol Med 3:95–101
5. Sanghi R, Verma P (2009) Biomimetic synthesis and characterization of protein capped silver nanoparticles. Bioresour Technol 100:501–504
6. Nazeruddin GM, Prasad NR, Waghmare SR, Garadkar KM, Mulla IS (2014) Extracellular biosynthesis of silver nanoparticle using *Azadirachta indica* leaf extract and its anti-microbial activity. J Alloys Compd 583:272–277
7. Murugan K, Panneerselvam C, Samidoss CM, Madhiyazhagan P, Suresh U, Roni M, Chandramohan B, Subramaniam J, Dinesh D, Rajaganesh R, Paulpandi M, Wei H, Aziz AT, Alsalhi MS, Devanesan S, Nicoletti M, Pavela R, Canale A, Benelli G (2016) *In vivo* and *in vitro* effectiveness of *Azadirachta indica*-synthesized silver nanocrystals against *Plasmodium berghei* and *Plasmodium falciparum*, and their potential against malaria mosquitoes. Res Vet Sci 106:14–22
8. Ajitha B, Reddy YAK, Reddy PS (2014) Biogenic nano-scale silver particles by Tephrosia purpurea leaf extract and their inborn antimicrobial activity. Spectrochim Acta Part A Mol Biomol Spectrosc 121:164–172
9. Kotakadi VS, Gaddam SA, Venkata SK et al (2016) Biofabrication and spectral characterization of silver nanoparticles and their cytotoxic studies on human CD34+ve stem cells. 3Biotech 6:216
10. Issaabadi Z, Nasrollahzadeh M, Sajadi SM et al (2017) Efficient catalytic hydration of cyanamides in aqueous medium and in the presence of Naringin sulfuric acid or green synthesized silver nanoparticles by using *Gongronema latifolium* leaf extract. J Colloid Interface Sci 503:57–67
11. Rao NH, Lakshmidevi N, Pammi SVN et al (2016) Green synthesis of silver nanoparticles using methanolic root extracts of *Diospyros paniculata* and their antimicrobial activities. Mater Sci Eng C 62:553–557
12. Suntar I, Akkol EK, Keles H et al (2012) Comparative evaluation of traditional prescriptions from *Cichorium intybus* L. for wound healing: stepwise isolation of an active component by in vivo bioassay and its mode of activity. J Ethnopharmacol 143:299–309
13. Syed NA, Hasan TN, Aalam SMM (2008) Evaluation of wound healing potential of *Cichorium intybus* L. (Asteraceae) in rats. Iranian J Pharm Ther 7:181–184
14. Sezik E, Tabata M, Yesilada E, Honda G, Goto K, Ikeshiro Y (1991) Traditional medicine in Turkey I. Folk medicine in Northeast Anatolia. J Ethnopharmacol 35:191–196
15. Nandagopal S, Kumari BDR (2007) Phytochemical and antibacterial studies of chicory (*Cichorium intybus* L.)—a multipurpose medicinal plant. Advan Biol Res 1:17–21
16. Bischoff TA, Nguyen-Dinh P, Arefi AG et al (2004) Antimalarial activity of Lactucin and Lactucopicrin: sesquiterpene lactones isolated from *Cichorium intybus* L. J Ethnopharmacol 95:455–457
17. Norbaek R, Nielsen K, Kondo T (2002) Anthocyanins from flowers of *Cichorium intybus*. Phytochemistry 60:357–359
18. Papetti A, Daglia M, Aceti C, Sordelli B, Spini V, Carazzone C, Gazzani G (2008) Hydroxycinnamic acid derivatives occurring in *Cichorium endivia* vegetables. J Pharma Biomed Anal 48:472–476
19. Mulinacci N, Innocenti M, Gallori S, Romani A, la Marca G, Vincieri FF (2001) Optimization of the chromatographic determination of polyphenols in the aerial parts of *Cichorium intybus* L. Chromatographia 54:455–461
20. Baghbani-Arani F, Movagharnia R, Sharifian A, Salehi S, Shandiz SAS (2017) Photo-catalytic, anti-bacterial, and anti-cancer properties of phyto-mediated synthesis of silver nanoparticles from *Artemisia tournefortiana* Rchb extract. J Photochem Photobiol Biol 173:640–649
21. Das S, Das J, Samadder A, Bhattacharyya SS, Das D, Khuda-Bukhsh AR (2013) Biosynthesized silver nanoparticles by ethanolic extracts of *Phytolacca decandra*, *Gelsemium sempervirens*, *Hydrastis canadensis* and *Thuja occidentalis* induce differential cytotoxicity through G2/M arrest in A375 cells. Colloids Surf B Biointerfaces 101:325–336
22. Alavi M, Karimi N (2017) Characterization, antibacterial, total antioxidant, scavenging, reducing power and ion chelating activities of green synthesized silver, copper and titanium dioxide nanoparticles using *Artemisia haussknechtii* leaf extract. Artif Cells Nanomed Biotechnol 12:1–16

23. Sadat Shandiz SA, Shafiee Ardestani M, Shahbazzadeh D, Assadi A, Ahangari Cohan R, Asgary V, Salehi S (2017) Novel imatinib loaded silver nanoparticles for enhanced apoptosis of human breast cancer MCF-7 cells. Art Cells Nanomed Biotechnol 45:1082–1091
24. Gallucci MN, Fraire JC, Ferreyra Maillard APV, Páez PL, Aiassa Martínez IM, Pannunzio Miner EV, Coronado EA, Dalmasso PR (2017) Silver nanoparticles from leafy green extract of Belgian endive (*Cichorium intybus* L. var. sativus): biosynthesis, characterization, and antibacterial activity. Mater Lett 197:98–101
25. Tripathi R, Kumar N, Shrivastav A et al (2013) Catalytic activity of biogenic silver nanoparticles synthesized by *Ficus panda* leaf extract. J Mol Catal B Enzym 96:75–80
26. Soshnikova V, Kim YJ, Singh P, Huo Y, Markus J, Ahn S, Castro-Aceituno V, Kang J, Chokkalingam M, Mathiyalagan R, Yang DC (2018) Cardamom fruits as a green resource for facile synthesis of gold and silver nanoparticles and their biological applications. Artif Cells Nanomed Biotechnol 46:108–117
27. Fröhlich E (2012) The role of surface charge in cellular uptake and cytotoxicity of medical nanoparticles. Int J Nanomedicine 7: 5577–5591
28. Abd Kelkawi AH, Kajani AA, Bordbar AK, (2017) Green synthesis of silver nanoparticles using *Mentha pulegium* and investigation of their antibacterial, antifungal and anticancer activity, 11:370–376
29. Keun HO, Veronika S, Josus M, et al. (2017) Biosynthesized gold and silver nanoparticles by aqueous fruit extract of *Chaenomeles sinensis* and screening of their biomedical activities. Artif Cells Nanomed Biotech. https://doi.org/10.1080/21691401.2017.1332636
30. Bethu MS, Netala VR, Domdi L, Tartte V, Janapala VR (2018) Potential anticancer activity of biogenic silver nanoparticles using leaf extract of *Rhynchosia suaveolens*: an insight into the mechanism, Artif Cells Nanomed Biotech https://doi.org/10.1080/21691401.2017.1414824, 1, 11
31. De Matteis V, Malvindi MA, Galeone A, Brunetti V, De Luca E, Kote S, Kshirsagar P et al (2015) Negligible particle-specific toxicity mechanism of silver nanoparticles: the role of Ag+ ion release in the cytosol. Nanomedicine 11:731–739
32. Huang C, Aronstam RS, Chen D, Huang Y (2010) Oxidative stress, calcium homeostasis, and altered gene expression in human lung epithelial cells exposed to ZnO nanoparticles. Toxicol in Vitro 24:45–55
33. Aceituno VC, Ahn S, Simu SY et al (2016) Silver nanoparticles from Dendropanax morbifera Léveille inhibit cell migration, induce apoptosis, and increase generation of reactive oxygen species in A549 lung cancer cells. In vitro Cell Dev Biol Animal 52:1012–1019
34. Fulda S (2009) Tumor resistance to apoptosis. Int J Cancer 124: 511–515
35. Green DR, Reed JC (1998) Mitochondria and apoptosis. Science 281:1309–1312
36. Kroemer G, Zamzami N, Susin SA (1997) Mitochondrial control of apoptosis. Immunol Today 8:44–51
37. Azandeh SS, Abbaspour M, Khodadadi A et al (2017) Anticancer activity of curcumin-loaded PLGA nanoparticles on PC3 prostate cancer cells. Iranian J Pharma Res 16:868–879
38. Maity P, Bepari M, Pradhan A, Baral R, Roy S, Maiti Choudhury S (2018) Synthesis and characterization of biogenic metal nanoparticles and its cytotoxicity and anti-neoplasticity through the induction of oxidative stress, mitochondrial dysfunction and apoptosis. Colloids Surf B: Biointerfaces 161:111–120
39. Aceituno VC, Abbai R, Moon SS et al (2017) *Pleuropterus multiflorus* (Hasuo) mediated straightforward eco-friendly synthesis of silver, gold nanoparticles and evaluation of their anti-cancer activity on A549 lung cancer cell line. Biomed Pharmacother 93: 995–1003
40. Banerjee PP, Bandyopadhyay A, Harsha SN et al (2017) *Mentha arvensis* (Linn.)-mediated green silver nanoparticles trigger caspase 9-dependent cell death in MCF7 and MDA-MB-231 cells. Breast Cancer (Dove Med Press) 18:265–278
41. Satchell P, Gutmann J, Witherspoon D (2003) Apoptosis: an introduction for the endodontist. Int Endod J 36:237–245
42. Elmore S (2007) Apoptosis: a review of programmed cell death. Toxicol Pathol 35:495–516
43. Wong RSY (2011) Apoptosis in cancer: from pathogenesis to treatment. J Exp Clin Cancer Res 30:87
44. Denault JB, Salvesen GS (2008) Apoptotic caspase activation and activity. Methods Mol Biol 414:191–220
45. Kamada S, Kikkawa U, Tsujimoto Y, Hunter T (2005) Nuclear translocation of caspase-3 is dependent on its proteolytic activation and recognition of a substrate-like protein(s). J Biol Chem 280: 857–860
46. Baharara J, Ramezani T., Hosseini N, et al. (2018) Silver nanoparticles synthesized coating with leaves *Zataria multiflora* extract induced apoptosis in HeLa cells through p53 activation, Iranian J Pharma Res. in press